Dynamic Monte-Carlo modeling of hydrogen isotope reactive–diffusive transport in porous graphite

R. Schneider [a,*], A. Rai [a], A. Mutzke [a], M. Warrier [b], E. Salonen [c], K. Nordlund [d]

[a] *Max-Planck-Institut für Plasmaphysik, D-17491 Greifswald, Germany*
[b] *Institute for Plasma Research, Gandhinagar, India*
[c] *Laboratory of Physics, HUT, P.O. Box 1100, FIN-02015, Finland*
[d] *Accelerator Laboratory, P.O. Box 43, University of Helsinki, FIN-00014, Finland*

Abstract

An equal mixture of deuterium and tritium will be the fuel used in a fusion reactor. It is important to study the recycling and mixing of these hydrogen isotopes in graphite from several points of view: (i) impact on the ratio of deuterium to tritium in a reactor, (ii) continued use of graphite as a first wall and divertor material, and (iii) reaction with carbon atoms and the transport of hydrocarbons will provide insight into chemical erosion. Dynamic Monte-Carlo techniques are used to study the reactive–diffusive transport of hydrogen isotopes and interstitial carbon atoms in a 3-D porous graphite structure irradiated with hydrogen and deuterium and is compared with published experimental results for hydrogen re-emission and isotope exchange.
© 2007 Published by Elsevier B.V.

1. Introduction

An equal mixture of deuterium and tritium will be the fuel used in a fusion reactor. It is important to study the recycling and mixing of these isotopes of hydrogen in graphite from several points of view: (i) impact on the ratio of deuterium to tritium in a reactor, (ii) continued use of graphite as a first wall and divertor material, and (iii) reaction with carbon atoms and the transport of hydrocarbons will provide insight into chemical erosion. The graphite

used in fusion devices as a first wall material is porous and consists of granules and voids.

These granules are typically 1–10 μm separated by voids which are typically a fraction of a micrometer. The granules consist of graphitic micro-crystallites of size 10–100 nm separated by micro-voids which are typically 1 nm (Fig. 1) [1–4]. These sub-structures, voids and microvoids provide a large internal surface area inside graphite where the hydrogen interstitial atoms can diffuse and react with each other which will affect the hydrogen isotope inventory and recycling behaviour and also chemical erosion. It is estimated that the trap site concentrations within the bulk graphite are of the order 10^{-3}–10^{-5} per C atom [5,6]. Graphites exposed to fusion edge plasmas also get damaged

* Corresponding author. Tel.: +49 3834 882400; fax: +49 3834 882409.
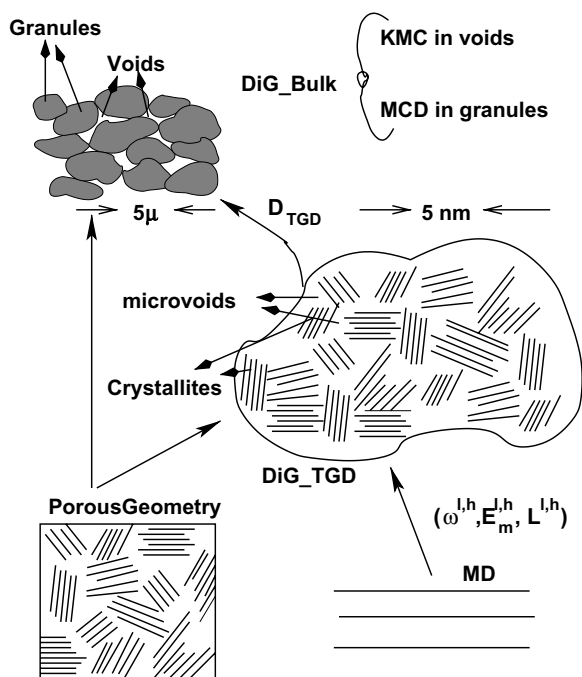 *E-mail address:* ralf.schneider@ipp.mpg.de (R. Schneider).

Fig. 1. Multiscale schematic. The acronyms used in the figure are MD (Molecular Dynamics), DiG (Diffusion in Graphite) and D_{TGD} (trans-granular diffusion coefficient). DiG$_{TGD}$ is the version of the multiscale code that handles trans-granular-diffusion and DiG$_{Bulk}$ is the version that handles bulk diffusion. Diffusion coefficients parametrized in terms of $E_m^{l,h}$ (two kinds of jumps having low- and high-migration energies (superscript l and h) are observed for H atom diffusing in crystalline graphite), $\omega l, h$ is the jump attempt frequencies for the corresponding jumps and $L^{l,h}$ is the corresponding jump distances.

by the incident energetic ions and neutrals from the plasma and this causes a high density of trap sites within the range of penetration of the incident ions ([2,5] and references therein).

2. Model

We use dynamic Monte-Carlo techniques to study the reactive–diffusive transport of hydrogen isotopes in a 3-D porous graphite structure irradiated with hydrogen and deuterium and compare with published experimental results for isotope exchange.

Incident hydrogen ions and neutrals which are not reflected have a wide range of possibilities as discussed in [1–3,7]. They can diffuse within the crystallite or along the crystallite surfaces or become trapped in the high density of traps region and become detrapped, or undergo chemical reactions to form hydrocarbons or recombine to form hydro-

gen molecules which can then diffuse along microvoids or voids.

The existence of such large variations in length scales of sub-structures coupled with the wide range of possible atomistic processes makes the study of hydrogen transport and inventory (or complementing this, the formation of hydrocarbons and their transport) in graphite a non-trivial exercise. Many detailed macroscopic models have been proposed to study hydrogen isotope inventory and transport in porous graphite [1–4] and hydrocarbon formation and transport in graphite [8]. These models use rate constants for transport from experiments [9–13,7], some of which still need theoretical explanations. There exists many microscopic models [14–17] using MD with either empirical potentials or density functional theory and they give insight into the microscopic mechanisms studied in graphite. It is desirable to use the insights gained from the microscopic models for modeling the transport in the mesoscale and further into the macroscale in order to understand the physical processes contributing to macroscopic transport.

We have earlier modeled hydrogen isotope diffusion in pure, crystal graphite using MD at microscales (2.5 nm, 10^{-10} s) and consistently parametrized the MD results within a KMC scheme [17]. A 3d, porous, granule structure was constructed using statistical distributions for crystallite dimensions and crystallite orientations for a specified microvoid fraction. The KMC scheme was extended to include trapping and detrapping at the crystallite–microvoid interface in the 3d porous granule structure to simulate trans-granular-diffusion (TGD) in the mesoscales (10^{-7}–10^{-6} m, several ms) [18] using the results from our microscale modeling and from experiments ([19] and references therein). Later, this concept was extended in our simulations to the macroscales (1 cm, up to a few seconds), thereby having a truly multiscale capability [20].

In this paper, we use an extension of this model. We introduce molecular species in addition to the atomic species to study the reactive–diffusive transport of hydrogen isotopes and interstitial carbon atoms in a 3-D porous graphite structure irradiated with hydrogen and deuterium. We compare the model results with published experimental results for re-emission and isotope exchange.

The parametrization of the processes for the molecules is based on [2]. Molecules in the crystallites can undergo a simple jump, characterized in terms

of the KMC parameters migration energy (2.0 eV), jump length (0.3 nm) and jump attempt frequency (2.74×10^{13} s^{-1} (typical phonon frequency)). Since it is very difficult for molecules to jump inside the parallel graphene planes due to their size, we intutively use migration energy of 2.0 eV (high enough as compared to energy needed by hydrogen molecules to jump in the voids). They can also experience a dissociation (4.45 eV, 0.2 nm, 2.74×10^{13} s^{-1}) [21]. Within the voids we consider simple jumps or desorption (0.06 eV, 1.0 nm, 1.0×10^{13} s^{-1}) or dissociation (4.45 eV, 0.2 nm, 1.0×10^{13} s^{-1}).

3. Re-emission of hydrogen

We initially create a cubic structure of 1×10^{-7} m representing one typical granule. $200 \times 200 \times 200$ cells are used with an elementary cell size of 0.5 nm. We consider a case of 2000 H atoms uniformly distributed in X–Y at a depth of 3.75×10^{-8} m along Z with a Gaussian distribution of width 7.8×10^{-9} m as calculated from TRIM runs of 1 keV hydrogen atoms impinging on carbon. Due to this short mean free path, modeling of one granule is sufficient for the re-emission studies.

In Fig. 2, the re-emitted flux for graphite with void fractions of 5%, 7% and 9% bombarded with 1 keV hydrogen ions are shown.

The simulation results follow the trends observed in the experiments [22] i.e., at lower temperatures hydrogen is re-emitted in the molecular form and at higher temperatures it is re-emitted in atomic form. It can be well explained following the model of Haasz et al. [2], where the re-emission process is basically governed by the competition between atom diffusion or desorption and recombination. The rise of the re-emission of atomic hydrogen at about 900 K is determined by the activation energy for entering the bulk. At these temperatures the diffusion within the granules is also quite low. Most of the transport is by surface diffusion of the solute atoms. Particles start getting into the bulk and from the bulk to the voids in our simulations at 1200 K.

The experimental results shows similar pattern with simulations for sample with 5% void fraction in our model. A little shift is observed in temperature for the onset of atomic hydrogen re-emission (T_{onset}) and consequently the temperature at which re-emitted flux of hydrogen atoms and molecules are equal (0.5) (T_{eq}). In order to demonstrate the sensitivity of T_{onset} and T_{eq} on the internal structure of sample, we have plotted the re-emission results for similar graphite samples having different trapping sites. Moreover from Fig. 2 it is evident that even by changing the void fraction to 7% T_{eq} shifts to higher temperatures (Fig. 3).

Increasing the void fraction to 9% with constant elementary void size, we observe that we get larger amounts of hydrogen molecules. As we increase the void fraction with same elementary void size we have more voids and lesser bulk elements, where a possible trapping of the atoms can happen (each bulk element is representing one microcrystal where
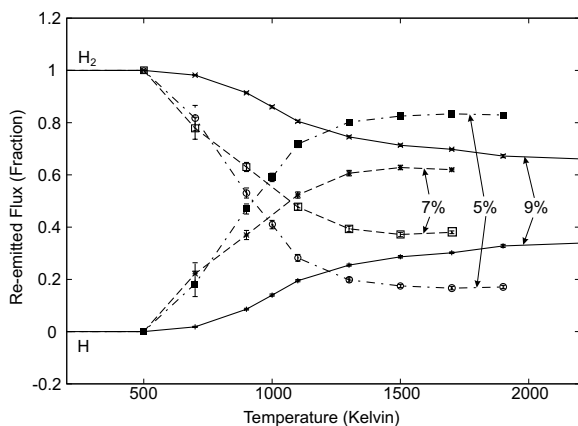

Fig. 2. Re-emitted flux of hydrogen atoms and molecules as a function of temperature for 5%, 7% and 9% voids. The elementary size of a void was in all the cases 5×10^{-9} m.
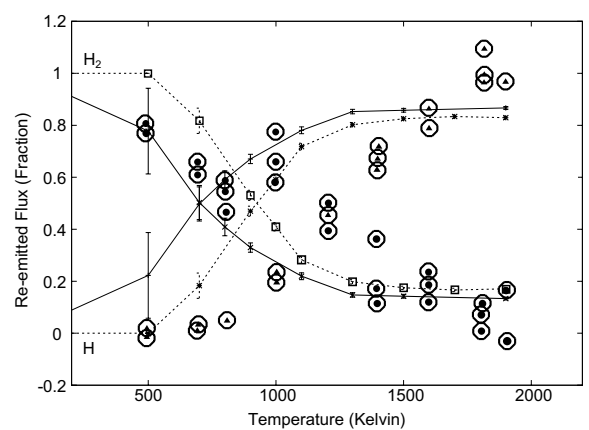

Fig. 3. Re-emitted flux of hydrogen atoms and molecules as a function of temperature. Bold triangle and circle enclosed in hexagons represents experimental data [22], solid lines shows simulation results for 5% void fraction with 4000 trap-sites and dotted lines represents simulation results for 5% voids with 2000 trap-sites. The elementary size of a void was in both cases 5×10^{-9} m.
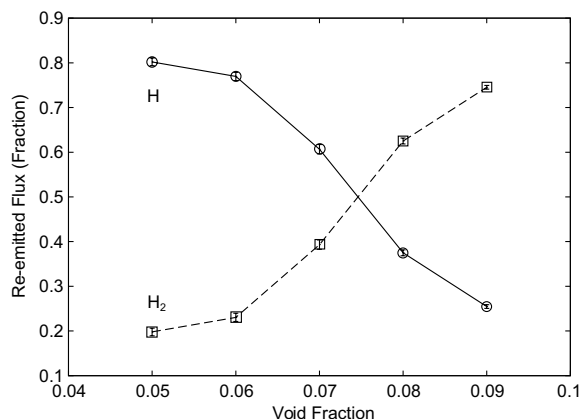
Fig. 4. Re-emitted flux of hydrogen atoms and molecules as a function of the void fraction at 1300 K. The elementary size of the voids was 5×10^{-9} m.
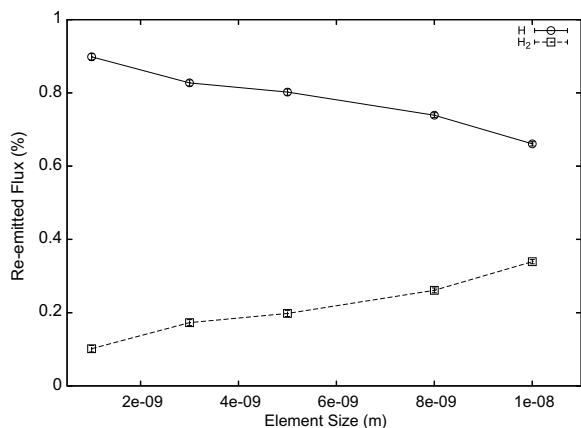

Fig. 5. Re-emitted flux of hydrogen atoms and molecules as a function of the elementary void size at 1300 K for a void fraction of 5%.

at its surface trapping/detrapping can occur). Therefore, more hydrogen molecule recombination events can occur and the molecular hydrogen flux increases (Fig. 4).

Changing the elementary void size and keeping the void fraction constant, Fig. 5 also shows an increase of the re-emitted hydrogen molecular flux with increasing elementary void size.

In this case, the system has less internal void surface with increasing elementary void size (small elementary voids create a large number of small voids, large elementary voids create a small number of large voids for a fixed void fraction). Therefore, less and less trapping/detrapping can occur at the void surfaces and more hydrogen molecular recombination events can happen.

4. Isotope exchange

To model isotope exchange experiments with simultaneous ion beam bombardment of hydrogen and deuterium (1 and 3 keV with gaussian depth-distributions with mean values of 2.75×10^{-8} and 5.95×10^{-8} m and standard deviations of 7.8×10^{-9} and 1.2×10^{-8} m), we used $280 \times 280 \times 280$ cells with an elementary cell size of 5.0×10^{-10} m resulting in a system size of 1.4×10^{-7} m. Runs were done at a temperature of 1000 K and for a microvoid size of 6.0×10^{-9} m. Deuterium molecules in the crystallites can undergo a simple jump, characterized in terms of the KMC parameters migration energy (2.0 eV), jump length (0.3 nm) and jump attempt frequency (2.74×10^{13} s^{-1}). Also, they can experience a dissociation (4.55 eV, 0.2 nm, 2.74×10^{13} s^{-1}). Within the voids we consider simple jumps or desorption (0.06 eV, 1.0 nm, 1.0×10^{13} s^{-1}) or dissociation (4.55 eV, 0.3 nm, 1.0×10^{13} s^{-1}). HD molecules can also jump within crystallites (2.0 eV, 0.3 nm, 2.74×10^{13} s^{-1}) or dissociate (4.51 eV, 0.2 nm, 2.74×10^{13} s^{-1}) [21]. Within the voids they can jump or desorb (0.06 eV, 1.0 nm, 1.0×10^{13} s^{-1}) or dissociate (4.51 eV, 0.2 nm, 1.0×10^{13} s^{-1}). The recombination distance for formation of molecules was taken as 0.2 nm [2].

For a void fraction of 7% steady-state conditions were reached after 1.2×10^{-8} s (Fig. 6). The relative fluxes of the modelling agree well with experiments [23].

To test the idea that the increase of hydrogen molecules observed experimentally at the beginning of the ion bombardment is due to microvoid crea-
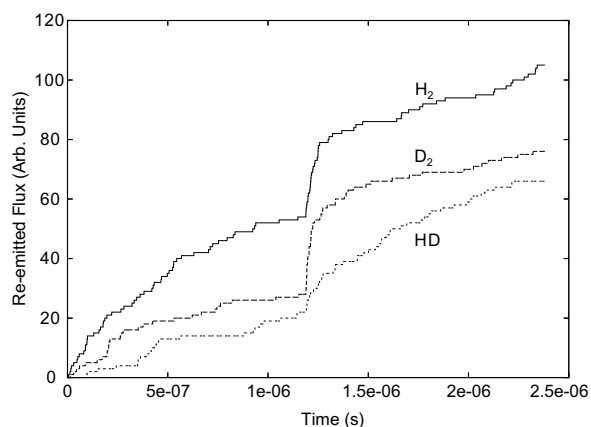

Fig. 6. Re-emitted flux of H$_2$, D$_2$ and HD molecules as a function of time.

tion, we continued the run after increasing the void fraction to 9%. A rise of both the hydrogen and deuterium molecular fluxes is seen due to the increase of the void surfaces as discussed before. However, the experimentally observed jump of hydrogen molecular fluxes followed by a slow decay to steady state combined with the slow rise of deuterium molecular fluxes is not reproduced. In the experiment, the ion-created microchannels are dominating the transport processes. In order to get better agreement with the experiment, the dynamics of this formation have to be included into the model. This is possible by adding to the time-step loop of our code one TRIM/TRIDYN calculation to determine the void distribution self-consistently in time.

5. Summary and conclusions

We have extended a multiscale scheme to model hydrogen transport in porous graphite to molecule formation and transport. The influence of the size and fraction of voids for 3-D porous graphite hydrogen re-emission was studied and agreed with existing models. The model should allow better quantative descriptions of these effects if the meso- and microstructure of the graphite is known. In case of isotope exchange an unresolved discrepancy remains between modeling and experiment, because hydrogen and deuterium molecules show similar trends in modeling, whereas the opposite time-dependencies of these molecules after activating ion beams are observed in experiments. Inclusion of TRIM/TRIDYN calculations for self-consistent calculation of the void distributions can eventually overcome this.

References

[1] Wolfhard Möller, J. Nucl. Mater. 162–164 (1989) 138.
[2] A.A. Haasz, P. Franzen, J.W. Davis, S. Chiu, C.S. Pitcher, J. Appl. Phys. 77 (1) (1995) 6.
[3] G. Federici, C.H. Wu, J. Nucl. Mater. 186 (1992) 131.
[4] A. Hassanein, B. Wiechers, I. Konkashbaev, J. Nucl. Mater. 258–263 (1998) 295.
[5] M. Mayer, M. Balden, R. Behrisch, J. Nucl. Mater. 252 (1998) 55.
[6] R.A. Causey, M.I. Baskes, K.L. Wilson, J. Vac. Sci. Technol. A 4 (3) (1986) 1189.
[7] J. Küppers, Surface Sci. Reports 22 (1995) 249.
[8] B.V. Mech, A.A. Haasz, J.W. Davis, J. Appl. Phys. 84 (3) (1998) 1655.
[9] B.M.U. Scherzer, M. Wielunski, W. Möller, A. Turos, J. Roth, Nucl. Instrum. and Meth. B 33 (1988) 714.
[10] B.M.U. Scherzer, J. Wang, W. Möller, J. Nucl. Mater. 162–164 (1989) 1013.
[11] W. Möller, B.M.U. Scherzer, J. Appl. Phys. 64 (1988) 4860.
[12] R.A. Causey, J. Nucl. Mater. 162–164 (1989) 151.
[13] H. Atsumi, S. Tokura, M. Miyake, in: Proceedings of 3rd International Conference on Fusion Reactor Materials, Karlsruhe, (1987), J. Nucl. Mater. 155–157 (1988) 241.
[14] E. Salonen, K. Nordlund, J. Keinonen, C.H. Wu, Phys. Rev. B 63 (2001), 195415–(1–14).
[15] Y. Ferro, F. Marinelli, A. Allouche, Chem. Phys. Lett. 368 (2003) 609.
[16] Y. Ferro, F. Marinelli, A. Allouche, J. Chem. Phys. 116#118 (2002) 8124.
[17] M. Warrier, R. Schneider, E. Salonen, K. Nordlund, Phys. Scripta T108 (2004) 85.
[18] M. Warrier, R. Schneider, E. Salonen, K. Nordlund, Contrib. Plasma Phys. 44#1–3 (2004) 307.
[19] K.L. Wilson et al., J. Nucl. Fusion 1 (1991) 31.
[20] M. Warrier, R. Schneider, E. Salonen, K. Nordlund, J. Nucl. Mater. 337–339 (2005) 580.
[21] G. Herzberg, Phys. Rev. Lett. 23 (1969) 1081.
[22] P. Franzen, E. Vietzke, J. Vac. Sci. Technol. A 12&13 (1994) 820.
[23] S. Chiu, A.A. Haasz, J. Nucl. Mater. 196–198 (1992) 972.